



Cite this: *CrystEngComm*, 2023, **25**, 48

Received 26th July 2022,
Accepted 24th October 2022

DOI: 10.1039/d2ce01026g

rsc.li/crystengcomm

Revealing uncommon transport in the previously unascertained very low cation clathrate-I $\text{Eu}_2\text{Ga}_{11}\text{Sn}_{35}^\dagger$

Wilarachchige D. C. B. Gunatilleke,^a Winnie Wong-Ng,^b Peter Y. Zavalij,^c Mingjian Zhang,^d Yu-Sheng Chen^d and George S. Nolas^{d,*a}

High occupancy of cation sites is typical for clathrate-I compositions allowing limited tunability of the electrical properties beyond doping and elemental substitution. Herein, we report on the structure and electrical transport of single-crystal $\text{Eu}_2\text{Ga}_{11}\text{Sn}_{35}$, the sole example of a very low (25%) cation concentration clathrate-I material with atypical transport directly attributable to the structure and stoichiometry.

Modification of the physical properties of materials can be realized *via* different doping strategies as well as alteration of the stoichiometry in certain compositions. In the latter case metal-to-semiconducting, semiconductor-to-insulating as well as metal-to-insulator transitions can be realized with stoichiometric variations.^{1–4} This approach can be applied to a wide variety of important applications of interest, including photovoltaics, thermoelectrics, magneto optics and magnetocaloric materials.^{5–8} Moreover, the pursuit of new materials employing new and unique synthetic approaches has impacted technological fields of interest.^{9–12} Nevertheless, molten metals employed as solvents, or fluxes, have been used for over a century in the pursuit of new compositions, as this synthesis approach allows for high diffusion rates at lower temperatures as compared to elemental reaction from the elements.¹³ In all these cases achieving an understanding of crystal structure and bonding, and their effects on the physical properties, is of primary importance and of fundamental interest.

A class of materials that continues to be of interest due to their diverse physical properties, as well as their potential for technological applications, is group-14 clathrates.¹⁴ One of the more engaging aspects of research on inorganic clathrates is in understanding the effects of cation occupancy, and how intermolecular and structural features modify the physical properties. This is particularly the case for low-cation concentrations. Although different compositions and structure types have been reported for some time,^{15,16} p-type semiconducting compositions are rare.^{17–23} One reason for this is the fact that clathrate-I compositions with low anion concentrations have not been realized. Thus, research on the synthesis, bonding and physical properties of inorganic clathrates has been primarily undertaken on electron-rich compositions motivated by the low thermal conductivity they possess and their potential as photovoltaic or thermoelectric materials.^{13,16,24–30} In electronic applications, thermoelectrics for example,³¹ both p and n-type materials of similar mechanical and physical properties, best obtained from like-structured materials, are required.

The clathrate-I crystal structure can be thought of as an open framework lattice formed by group-14 elements that is comprised of two dodecahedra and six tetrakaidecahedra per cubic unit cell with “guest” atoms residing inside these polyhedra formed by the framework. There are scarce reports on less-than-full cation occupancy clathrate-I compositions, and none on very low cation concentration compositions.^{14,32–35} Although reports on the synthesis of very low cation concentration clathrate-II compositions have been published, *e.g.* $\text{Na}_x\text{Si}_{136}$,^{36–40} there have not been any reports on very low cation concentration clathrate-I compositions. The thermal conductivity of these materials is expected to be low,^{14,17,25,29} however, the salient aspects of our work reveal that p-type semiconducting $\text{Eu}_2\text{Ga}_{11}\text{Sn}_{35}$ displays atypical electronic transport that is a direct result of the structure and

^a Department of Physics, University of South Florida, Tampa, FL 33620, USA.

E-mail: gnolas@usf.edu

^b Materials Measurement Science Division, National Institute of Standards and Technology, Gaithersburg, MD 20899, USA

^c Department of Chemistry and Biochemistry, University of Maryland, College Park, MD 20742, USA

^d ChemMatCARS, University of Chicago, Argonne, IL 60439, USA

† Electronic supplementary information (ESI) available. CCDC 2154399. For ESI and crystallographic data in CIF or other electronic format see DOI: <https://doi.org/10.1039/d2ce01026g>

composition in this very low cation concentration clathrate-I composition.

Single crystals of $\text{Eu}_2\text{Ga}_{11}\text{Sn}_{35}$ were grown from Sn flux. Europium pieces (99.99%, Ames Labs), Ga pellets (99.99999%, Alfa Aesar) and Sn pieces (99.99999%, Alfa Aesar)⁴¹ in a 1:2:12 atomic ratio were loaded into a tungsten crucible that was then sealed inside a glass tube, all synthetic procedures occurring inside a nitrogen glovebox. The glass tube was sealed under vacuum, heated to 650 °C at a rate of 25 degrees per hour, where it was held for 15 hours before slow cooling to 450 °C at a rate of 10 degrees per hour at which point it was air cooled to room temperature. A mixture of 10 mL HCl, 10 mL HNO_3 and 80 mL DI water was used to remove potential residual flux from the surface of the $\text{Eu}_2\text{Ga}_{11}\text{Sn}_{35}$ crystals. Several single crystals were preliminarily investigated by X-ray diffraction (XRD) employing a Bruker Smart Apex II CCD diffractometer using Mo K_α radiation. Single-crystal synchrotron data was collected with a Huber 3-circles diffractometer equipped with a Pilatus3 X 1M CdTe detector employing ChemMatCARS advanced crystallography program at the Advanced Photon Source (APS) of Argonne National Laboratory with applied absorption corrections using the Brennan method.⁴⁵ Fig. 1 illustrates the crystal structure. The structure was solved with the ShelXT-2014⁴³ program and refined with ShelXL-2018/3.⁴⁴ Temperature-dependent electrical transport measurements were performed on a single crystal employing the Physical Property Measurements System from Quantum Design. Further structural and measurement details are provided in the ESI.†

The Hall concentration, p , at room temperature ($5.90 \times 10^{18} \text{ cm}^{-3}$) was much less than that expected by simple electron counting ($4 \times 10^{21} \text{ cm}^{-3}$) assuming the Zintl rule

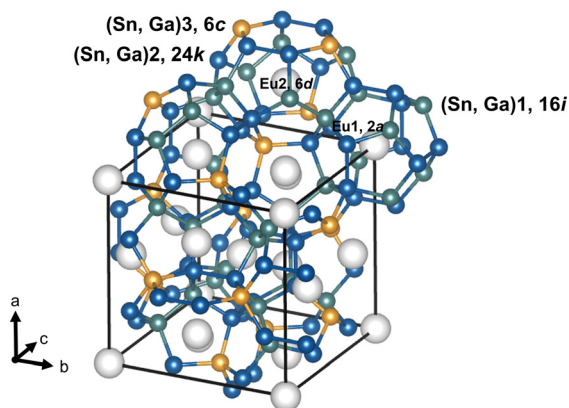


Fig. 1 The $\text{Eu}_2\text{Ga}_{11}\text{Sn}_{35}$ crystal structure emphasizing the clathrate-I framework $(\text{Sn}/\text{Ga})_{20}$ and $(\text{Sn}/\text{Ga})_{24}$ polyhedra. The 6c (yellow), 16i (green) and 24k (dark blue) Wyckoff sites are labelled, Sn and Ga randomly occupy all three framework sites. The structure crystallizes in the space group $Pm\bar{3}n$ with a lattice parameter of 11.9497(5) Å, as determined by single crystal synchrotron data.⁴² The unit cell of the structure (highlighted by black solid lines) contains Eu at the 2a and 6d sites in a 1:3 ratio, respectively. The sites of possible occupancy by Eu are displayed by light grey spheres.

with Eu providing two electrons to the framework and Ga and Sn providing three and four valence electrons, respectively. Moreover, our resistivity, ρ , measurements suggest transport *via* variable-range hopping (VRH) that is indicative of impurity-band conduction, as shown in Fig. 2(a). The fit to $\rho = \rho_0 \exp[(T_0/T)^{1/4}]$ in the figure indicates a transition from band conduction to impurity-band conduction at approximately 120 K. Hence, both valence band conduction as well as a low-mobility impurity band acceptor density, N_a , is required to describe the hole transport in $\text{Eu}_2\text{Ga}_{11}\text{Sn}_{35}$.^{46,47} Our model, which includes an impurity band with N_a at energy ε_a above the valence-band edge, describes the transport data very well as discussed in what follows and shown in Fig. 2.

For hole transport the equation for charge neutrality is

$$N_a - n_a = p, \quad (1)$$

where n_a is the acceptor impurity atom density.^{40,41} The valence band mobility (μ) and n_a can be solved simultaneously using the expressions given for R_H and ρ , namely

$$R_H = \frac{1}{e} \frac{p\mu^2 + n_a\mu_a^2}{(p\mu + n_a\mu_a)^2} \quad \text{and} \quad (2)$$

$$\rho = \frac{1}{e(p\mu + n_a\mu_a)} \quad (3)$$

As shown in Fig. 2(b)–(d), excellent agreement to the experimental Hall coefficient, R_H , ρ , and Seebeck coefficient, S_{tot} , data were obtained using these expressions with $\mu_a = 0.06 \text{ cm}^2 \text{ V}^{-1} \text{ s}^{-1}$ in order to simplify the simultaneous analysis of all the experimental data according to the model. A weighted sum of S_{tot} was used with contributions from the valence band (S) and impurity band (S_a) given by,

$$S_{\text{tot}} = \frac{Sp\mu + S_a n_a \mu_a}{p\mu + n_a \mu_a} \quad \text{and} \quad (4)$$

$$S = \frac{k_B}{e} \left(\frac{2 + v}{1 + v} \frac{F_{1+v}(\eta)}{F_v(\eta)} - \eta \right) \quad (5)$$

where $\eta = \zeta_F/k_B T$, ζ_F is the chemical potential measured with respect to the band edge and v is a constant value that is governed by the dominant scattering mechanism ($v = 2, 0.5$ and 0 for ionized impurity, neutral impurity, and acoustic phonon scattering, respectively). Eqn (4) simplifies to $S_{\text{tot}} \approx S(1 + n_a\mu_a/p\mu)^{-1}$ since $S \gg S_a$ at all temperatures other than very low temperatures. As shown in Fig. 2 the fits agree very well with the experimental values when ionized impurity scattering ($v = 2$) is dominant throughout the entire temperature range of the R_H data. A comparison between the temperature dependent μ values obtained from the model and temperature dependent forms of hall mobility for ionized impurity scattering ($\sim T^{-3/2}$), neutral impurity ($\sim \text{const}$) and acoustic phonon scattering ($\sim T^{-3/2}$) at the different v

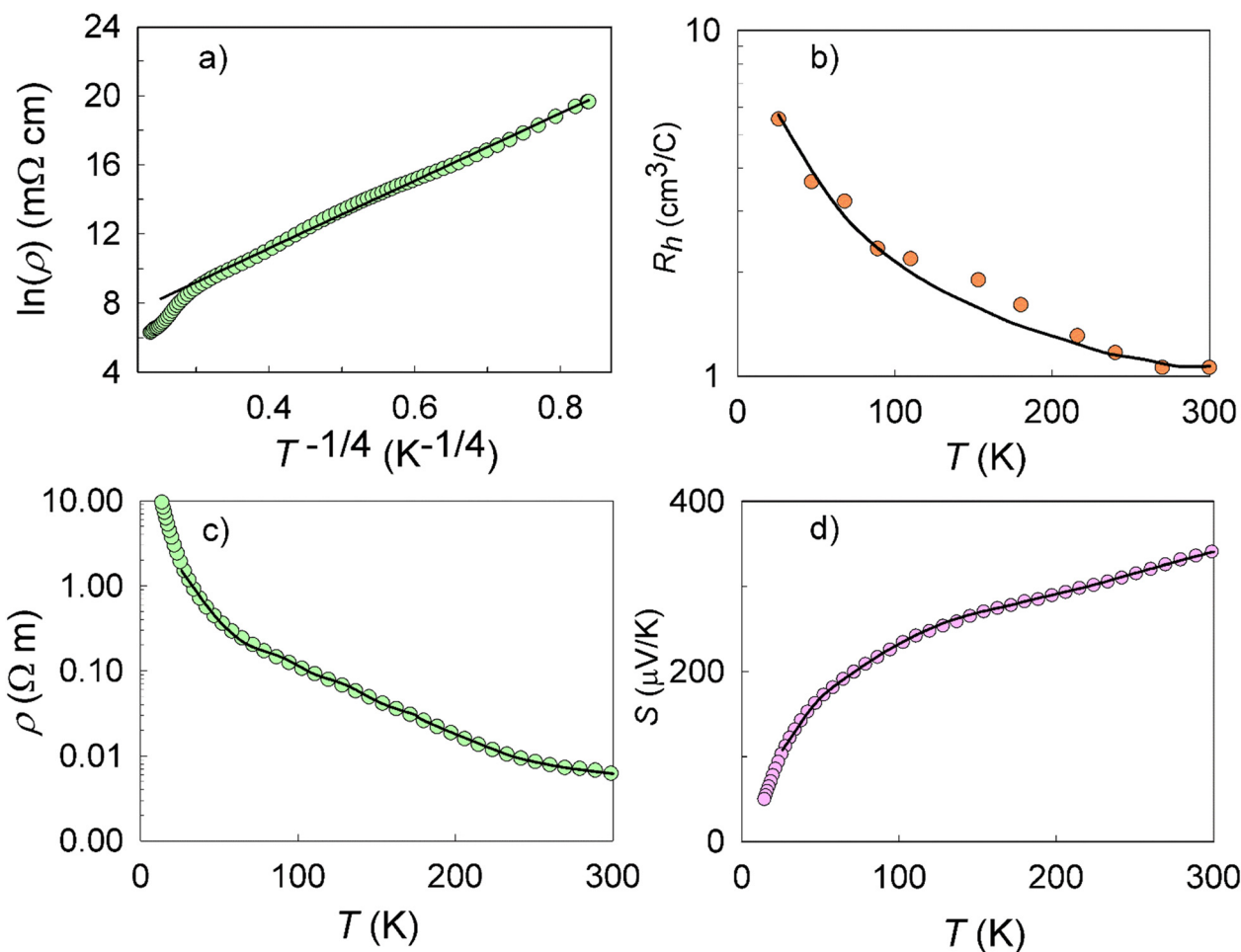


Fig. 2 (a) $\ln(\rho)$ vs. $1/T^{1/4}$, where the solid line is a fit of the form $\rho = \rho_0 \exp[(T_0/T)^{1/4}]$ with $\rho_0 = 2.84 \times 10^{-2} \Omega \text{ cm}$ and $T_0 = 1.46 \times 10^5 \text{ K}$. At room temperature $\rho = 620 \text{ m}\Omega \text{ cm}$. Note the ESI† where the data indicates a 0.13 eV bandgap for $\text{Eu}_2\text{Ga}_{11}\text{Sn}_{35}$. Temperature-dependent (b) Hall coefficient, (c) resistivity and (d) Seebeck coefficient data with solid lines from the model described in the text.

values described above confirmed this observation. These results also indicate the self-consistency of the model. At $\nu = 2$ the expressions,

$$p = N_a \left[1 + \frac{1}{2} \exp\left(\eta - \frac{\epsilon_a}{k_B T}\right) \right]^{-1}, \quad (6)$$

$$p = \frac{4\pi(2m_e k_B T)^{3/2}}{h^3} \left(\frac{m^*}{m_e}\right)^{3/2} F_{1/2}(\eta) \quad \text{and} \quad (7)$$

$$F_r = \int_0^\infty \frac{x^r}{1 + e^{x-\eta}} dx \quad (8)$$

can be employed to calculate m^* and ϵ_a using η and N_a derived above resulting in $\mu = 1.7 \text{ cm}^2 \text{ V}^{-1} \text{ s}^{-1}$, $m^* = 0.38m_e$ and $N_a = 5.91 \times 10^{18} \text{ cm}^{-3}$ at $\epsilon_a = 1.6 \text{ meV}$ above the valence band edge at room temperature. Here, m^* is the hole effective mass, m_e is the free electron mass and F_r is the Fermi integral of order r . This m^* value is small, as is also the case for n-type clathrate-I compositions and reveals the relatively steep curvature of the valence band, with an acceptor density that reveals the ‘balance’ between the

europium ion donors and compensation from the framework acceptors as N_a is smaller than that reported for n-type clathrate-I compositions.¹⁴

In summary, single-crystal $\text{Eu}_2\text{Ga}_{11}\text{Sn}_{35}$ was grown from tin flux allowing for intrinsic temperature-dependent electrical properties measurements and analyses. Atypical electrical transport, as compared with other clathrate compositions, is obtained for this very low cation tin clathrate-I material with transport data indicating conduction band to impurity band conduction with decreasing temperature. Our model, as described in detail above, fits the transport data very well. Our work also reinforces the impact of metallic flux crystal growth in new materials research.

The authors acknowledge financial support from the U.S. National Science Foundation (NSF) under Grant No. DMR-1748188. W. W.-N. thanks H. Jores for work during the preliminary structure study. ChemMatCARS Sector 15 was principally supported by the Divisions of Chemistry (CHE) and Materials Research (DMR), National Science Foundation, under grant number NSF/CHE-1834750. Use of the Advanced Photon Source, an Office of Science User Facility operated for

the U.S. Department of Energy (DOE) Office of Science by Argonne National Laboratory, was supported by the U.S. DOE under Contract No. DE-AC02-06CH11357.

Author contributions

Wilarachchige D. C. B. Gunatilleke: investigation, formal analysis, visualization. Winnie Wong-Ng: data curation, formal analysis. Peter Y. Zavalij: data curation. Mingjian Zhang: data curation. Yu-Sheng Chen: data curation, formal analysis. George S. Nolas: conceptualization, investigation, supervision, writing – original draft, project administration.

Conflicts of interest

There are no conflicts to declare.

Notes and references

- J. M. Honig and L. L. V. Zandt, *Annu. Rev. Mater. Sci.*, 1975, **5**, 225.
- S. Stefanoski, C. D. Malliakas, M. G. Kanatzidis and G. S. Nolas, *Inorg. Chem.*, 2012, **51**, 8686.
- C. H. Griffiths and H. K. Eastwood, *J. Appl. Phys.*, 1974, **45**, 2201.
- D. S. Jeong, R. Thomas, R. S. Katiyar, J. F. Scott, H. Kohlstedt, A. Petraru and C. S. Hwang, *Rep. Prog. Phys.*, 2012, **75**, 076502.
- J. He and T. M. Tritt, *Science*, 2017, **357**, eaak9997.
- K. Tsevas, J. A. Smith, V. Kumar, C. Rodenburg, M. Fakis, A. R. B. Mohd Yusoff, M. Vasilopoulou, D. G. Lidzey, M. K. Nazeeruddin and A. D. Dunbar, *Chem. Mater.*, 2021, **33**, 554.
- J. Y. Rhee, Y. V. Kudryavtsev and Y. P. Lee, *Phys. Rev. B: Condens. Matter Mater. Phys.*, 2003, **68**, 045104.
- A. De Campos, D. L. Rocco, A. M. G. Carvalho, L. Caron, A. A. Coelho, S. Gama, L. M. Da Silva, F. C. Gandra, A. O. Dos Santos, L. P. Cardoso and P. J. Von Ranke, *Nat. Mater.*, 2006, **5**, 802.
- S. Stefanoski, M. Beekman, W. Wong-Ng, P. Zavalij and G. S. Nolas, *Chem. Mater.*, 2011, **23**, 1491.
- L. Ye, S. Zhang, L. Huo, M. Zhang and J. Hou, *Acc. Chem. Res.*, 2014, **47**, 1595.
- B. G. Shen, J. R. Sun, F. X. Hu, H. W. Zhang and Z. H. Cheng, *Adv. Mater.*, 2009, **21**, 4545.
- M. G. Kanatzidis, *Curr. Opin. Solid State Mater. Sci.*, 1997, **2**, 139.
- M. G. Kanatzidis, R. Pöttgen and W. Jeitschko, *Angew. Chem., Int. Ed.*, 2005, **44**, 6996.
- G. S. Nolas, *The physics and chemistry of inorganic clathrates*, Springer, vol. 199, 2014.
- C. Cros, M. Pouchard and P. Hagenmuller, *C. R. Hebd. Seances Acad. Sci.*, 1965, **260**(18), 4764.
- J. S. Kasper, P. Hagenmuller, M. Pouchard and C. Cros, *Science*, 1965, **150**, 1713.
- G. S. Nolas, G. A. Slack and S. B. Schujman, in *Semiconductors and Semimetals*, ed. T. M. Tritt, Academic Press, 2001, vol. 69, pp. 255–300.
- C. Candolfi, U. Aydemir, M. Baitinger, N. Oeschler, F. Steglich and Y. Grin, *J. Appl. Phys.*, 2012, **111**, 043706.
- S. Deng, X. Tang and Q. Zhang, *J. Appl. Phys.*, 2007, **102**, 043702.
- H. Zhang, H. Borrmann, N. Oeschler, C. Candolfi, W. Schnelle, M. Schmidt, U. Burkhardt, M. Baitinger, J. T. Zhao and Y. Grin, *Inorg. Chem.*, 2011, **50**, 1250.
- S. Deng, X. Tang, P. Li and Q. Zhang, *J. Appl. Phys.*, 2008, **103**, 073503.
- N. Jaussaud, P. Gravereau, S. Pechev, B. Chevalier, M. Ménétrier, P. Dordor, R. Decourt, G. Goglio, C. Cros and M. Pouchard, *C. R. Chim.*, 2005, **8**, 39.
- K. Wei, A. R. Khabibullin, D. Hobbs, W. Wong-Ng, T. Chang, S. G. Wang, I. Levin, Y. S. Chen, L. M. Woods and G. S. Nolas, *Inorg. Chem.*, 2018, **57**, 9327.
- J. F. Meng, N. V. Chandra Shekar, J. V. Badding and G. S. Nolas, *J. Appl. Phys.*, 2001, **89**, 1730.
- G. S. Nolas, J. L. Cohn, G. A. Slack and S. B. Schujman, *Appl. Phys. Lett.*, 1998, **73**, 178.
- M. Beekman and G. S. Nolas, *J. Mater. Chem.*, 2008, **18**, 842.
- G. B. Adams, M. O'Keefe, A. A. Demkov, O. F. Sankey and Y.-M. Huang, *Phys. Rev. B: Condens. Matter Mater. Phys.*, 1994, **46**, 8048.
- X. Blase, P. Gillet, A. San Miguel and P. Mélinon, *Phys. Rev. Lett.*, 2004, **92**, 21550.
- G. S. Nolas and G. A. Slack, *Am. Sci.*, 2001, **89**, 136.
- A. P. Wilkinson, C. Lind, R. A. Young, S. D. Shastri, P. L. Lee and G. S. Nolas, *Chem. Mater.*, 2002, **14**, 1300.
- G. S. Nolas, J. Sharp and J. Goldsmid, *Thermoelectrics Basic Principles and New Materials Developments*, Springer, 2001.
- B. Böhme, A. Guloy, Z. Tang, W. Schnelle, U. Burkhardt, M. Baitinger and Y. Grin, *J. Am. Chem. Soc.*, 2007, **129**, 5348.
- G. K. Ramachandran, P. F. McMillan, J. Dong and O. F. Sankey, *J. Solid State Chem.*, 2000, **154**, 626.
- A. Wosylus, I. Veremchuk, W. Schnelle, M. Baitinger, U. Schwarz and Y. Grin, *Chem. – Eur. J.*, 2009, **15**, 5901.
- D. Machon, P. Toulemonde, P. F. McMillan, M. Amboage, A. Munoz, P. Rodríguez-Hernández and A. San Miguel, *Phys. Rev. B: Condens. Matter Mater. Phys.*, 2009, **79**, 184101.
- G. K. Ramachandran, J. Dong, J. Diefenbacher, J. Gryko, R. F. Marzke, O. F. Sankey and P. F. McMillan, *J. Solid State Chem.*, 1999, **145**, 716.
- G. S. Nolas, M. Beekman, J. Gryko, G. A. Lamberton Jr, T. M. Tritt and P. F. McMillan, *Appl. Phys. Lett.*, 2003, **82**, 910.
- A. Ammar, C. Cros, M. Pouchard, N. Jaussaud, J. M. Bassat, G. Villeneuve, M. Duttine, M. Ménétrier and E. Reny, *Solid State Sci.*, 2004, **6**, 393.
- M. Beekman and G. S. Nolas, *Phys. B*, 2006, **383**, 111.
- M. Beekman, E. N. Nenghabi, K. Biswas, C. W. Myles, M. Baitinger, Y. Grin and G. S. Nolas, *Inorg. Chem.*, 2010, **49**, 5338.
- Certain trade names and company products are mentioned in the text or identified in illustrations in order to adequately specify the experimental procedures and equipment used. In no case does such identification imply recommendation or endorsement by the National Institute of Standards and Technology.

- 42 CCDC 2154399 contains the supplementary crystallographic data for this paper.
- 43 G. M. Sheldrick, *Acta Crystallogr., Sect. A: Found. Adv.*, 2014, **70**, C1437.
- 44 G. M. Sheldrick, *Acta Crystallogr., Sect. C: Struct. Chem.*, 2015, **17**, 3.
- 45 S. Brennan and P. L. Cowan, *Rev. Sci. Instrum.*, 1991, **63**, 850.
- 46 B. M. Askerov, *Electron Transport Phenomena in Semiconductors*, World Scientific, Singapore, 1994, p. 60.
- 47 J. S. Blakemore, *Semiconductor statistics*, Courier Corporation, 2002, p. 117.